Journal of Membrane Science 713 (2025) 123347

Contents lists available at ScienceDirect

Journal of Membrane Science

journal homepage: www.elsevier.com/locate/memsci

Micropollutant removal via nanofiltration: The effect of salt concentration — Theory and experimental validation

S. Castaño Osorio [a,b], I.I. Ryzhkov [c,d], E. Spruijt [e], A. van der Wal [b,f], P.M. Biesheuvel [a], J.E. Dykstra [b,*]

[a] Wetsus, European Centre of Excellence for Sustainable Water Technology, Oostergoweg 9, 8911 MA Leeuwarden, The Netherlands
[b] Environmental Technology, Wageningen University & Research, Bornse Weilanden 9, 6708 WG Wageningen, The Netherlands
[c] Institute of Computational Modeling SB RAS, Akademgorodok 50-44, 660036 Krasnoyarsk, Russia
[d] Siberian Federal University, Svobodny 79, 660041 Krasnoyarsk, Russia
[e] Institute for Molecules and Materials, Radboud University, Heyendaalseweg 135, 6525 AJ Nijmegen, The Netherlands
[f] Evides Water Company, Schaardijk 150, 3063 NH Rotterdam, The Netherlands

ARTICLE INFO

Keywords:
Micropollutant rejection
Nanofiltration
Solution friction
Modeling

ABSTRACT

Nanofiltration guarantees high water recovery and low energy consumption in removing micropollutants (MPs). In this study, we derive a concise model to describe MP removal with nanofiltration membranes. We compare the results from the model with experimental data for the removal of 7 MPs with 5 salt concentrations using the NF270 membrane. Our findings indicate that the model accurately describes MP transport through nanofiltration membranes. Furthermore, we evaluate the effect of salt concentration on MP rejection. The results show that salt concentration impacts MP rejection differently based on MP charge and size. Increasing salt concentration decreases the rejection of counter-charged MPs that are small and increases the rejection of counter-charged MP that are large.

1. Introduction

Reverse osmosis (RO) and nanofiltration (NF) are leading technologies in the production of drinking water. In RO, the membranes provide a superior ion rejection. Therefore, RO membranes are used for seawater and brackish water desalination [1–3]. Conversely, NF membranes exhibit lower ion rejection compared to RO membranes. However, NF membranes are efficient in removing larger molecules such as organic matter and (organic) micropollutants (MPs) [4,5]. For MP removal, NF is often considered as an alternative to RO because of the higher water recovery, which is the ratio of the purified water that is produced over the feed water that is consumed, along with the lower energy requirements. Compared to RO, NF membranes have a higher porosity and larger pores which allows higher water and solute fluxes.

To predict and understand the removal of micropollutants (MPs) using nanofiltration under various conditions, accurate transport models are required. Several models have been proposed to study and understand the transport and rejection of MPs using membranes. For instance, Kim et al. implemented a modeled to compare the contributions of diffusion and convection to the transport of pharmaceuticals and disinfection by-products [6]. Nghiem et al. studied the effect of steric exclusion on rejection and used a hydrodynamic approach to model the transport of neutral MPs through cylindrical pores [7]. Wang et al. investigated the rejection and transport of neutral and charged MPs using the Donnan Steric Pore Model & Dielectric Effect (DSPM&DE) model [8]. Moreover, other researchers have also addressed the effects of physico-chemical phenomena on the rejection of MPs and proposed models to include these phenomena. For instance, some studies have focused on the effects of solute–membrane interactions on the rejection of MPs [9–11] as well as the effects of biofouling [12].

Although several studies have focused on implementing and extending existing models to study MP removal, some of these models remain complex, mostly because multiple fitting parameters are required to capture all the different properties of the MP and the membrane. There is a need for a model that captures the key transport mechanisms: diffusion, convection, and electromigration, and that is easy to implement, allowing for comparison with experimental datasets on membrane performance. Such a model has been developed based on solution-friction (SF) theory and has been compared with data sets for highly charged and uncharged reverse osmosis (RO) membranes [13]. Our goal is to extend this simple model to nanofiltration (NF) and include the removal of MPs. The extended model will allow for accurate

* Corresponding author.
E-mail address: jouke.dykstra@wur.nl (J.E. Dykstra).

https://doi.org/10.1016/j.memsci.2024.123347
Received 25 June 2024; Received in revised form 13 September 2024; Accepted 17 September 2024
Available online 21 September 2024
0376-7388/© 2024 The Authors. Published by Elsevier B.V. This is an open access article under the CC BY license (http://creativecommons.org/licenses/by/4.0/).

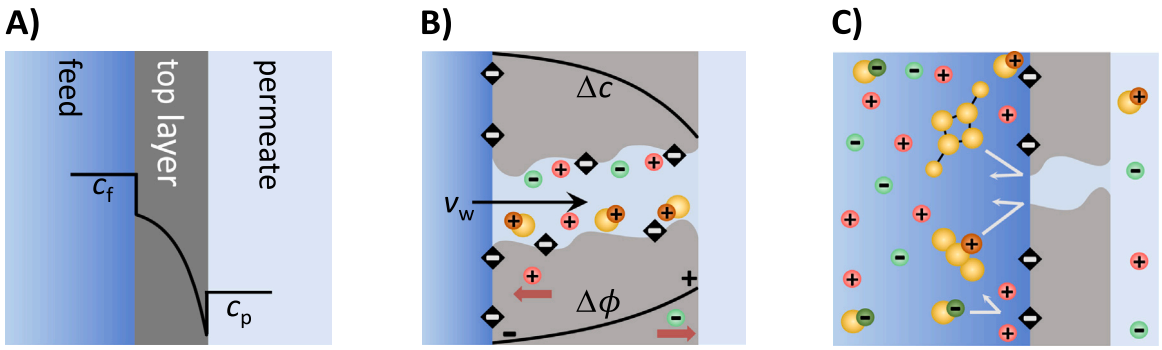

Fig. 1. Overview of the phenomena considered to study the removal of MPs. (A) On both sides of the membrane, the size and charge of the solute affect the partitioning equilibria between membrane and solutes. Concentration c_f is of the solute in the feed and c_p in the permeate. (B) The flux of solutes across the membrane is the result of diffusion due to concentration gradients, Δc, electromigration, due to potential differences, $\Delta\phi$, and convection due to water flux, v_w. (C) Solutes are rejected by the membrane due to steric and charge exclusion.

prediction of MP removal and can be used to assess the performance of NF modules and further improve water purification processes.

In this study, we introduce a novel equation for MP flux and rejection in NF processes. This equation can estimate rejection without complex numerical solutions, making it particularly advantageous for designing treatment processes in real-life applications. Implementing this equation is straightforward, requiring only two parameter values for each MP that is considered: the mass transfer coefficient within the membrane and a characteristic transport parameter unique to each MP and specific membrane. These parameters can be determined through standard filtration experiments conducted at the laboratory scale. Accurate identification of these parameters facilitates realistic prediction of MP rejection.

In addition to developing this novel equation, we conducted filtration experiments with 7 micropollutants to estimate the model parameters that yielded accurate predictions of MP rejection. The model was employed to investigate the impact of salt concentration on MP rejection and to explore the relevance of charge exclusion and electromigration for MP rejection.

The model in the present work is based on the SF theory and considers the partitioning of solutes at the membrane–solution interface and the transport due to diffusion, convection, and electromigration. Two assumptions are incorporated in the model; first, the MPs are trace solutes that do not affect the removal of the main solutes present at high concentrations, which are the salt ions; and second, the potential ϕ_m across the membrane is independent of the MP concentration in the membrane, which can also be justified by the relatively low concentrations (compared to the salt ions) of the MPs. The model results in a modified Hertz equation for the flux of MPs through the membrane that is dependent on the potential difference across the membrane. In the model, this potential difference is solely affected by the rejection of the salt ions. Furthermore, we defined a modified Peclet number, which captures the operational conditions, and a transport number that is characteristic to each micropollutant for a specific membrane. An overview of phenomena that are included in our model is depicted in Fig. 1; namely, solute partitioning at the membrane–solution interface, size and charge based rejection, and transport through the membrane pores due to diffusion, convection, and electromigration.

Experiments were conducted to validate the proposed model and compare theoretical calculations with the rejection data of 7 MPs. Within the experimental work, we explore the impact of salt concentration on the removal of MPs. Generally, the effect of salt concentration on removal has been associated with electrostatic interactions [14,15]. For instance, Nghiem et al. studied the effect of NaCl concentration on the rejection of ibuprofen and sulfamethoxazole, finding that increasing salt concentration decreases the removal of both micropollutants [16]. Similarly, Rutten et al. investigated the effect of salt concentration and dominant salt on the removal of MPs with hollow fiber nanofiltration membranes [17]. They found that the effect of salt concentration on MP removal depends on the charge of the MP, the type of membrane used, and the dominant salt in solution. In terms of modeling, Fini et al. used a purely steric model to study the effect of water matrix on the rejection of pesticides [18], while Rutten et al. employed the Donnan steric pore model, including dielectric exclusion, to qualitatively predict the removal of 4 micropollutants [17].

In summary, the present manuscript introduces a model designed to analyze and predict micropollutant removal via NF. We present a detailed derivation of the model and a comparison with experimental data to establish its validity. Furthermore, this work explores the impact of salt concentration on the removal efficiency of several micropollutants. Through this research, we aim to advance our understanding of MP removal with NF.

2. Theory

2.1. Micropollutant rejection

In this section, we outline the theoretical framework for the removal of MPs with NF membranes. From this point onward, we will use the term rejection instead of removal. Based on the SF theory, we derive transport equations to determine the flux and rejection of MPs. The resulting equations capture the effects of operating conditions, ionic strength, and the intrinsic properties of both the MPs and the membranes on MP rejection. We consider charged and neutral MPs. The theoretical framework relies on the extended Nernst–Planck (ENP) equation, describing the flux of MPs by convection, diffusion, and electromigration

$$J_i = K_{f,i} c_i v_w - K_{f,i} k_{m,i} \left(\frac{\partial c_i}{\partial x} + z_i c_i \frac{\partial \phi}{\partial x} \right) \quad (1)$$

where the friction factor $K_{f,i}$ represents the friction of MPs with the membrane matrix, c_i is the concentration of MPs, and v_w is the transmembrane water flux in m/s which can be translated to a unit L/m^2/h, commonly abbreviated as LMH. The transmembrane water flux depends on the water permeability of the membrane A_m in LMH/bar, salt concentration, and operating pressure. In the SI, we present the equation used to determine v_w. The mass transfer coefficient is given by $k_{m,i} = D_i \epsilon / L_m$ (LMH), where D_i is the diffusion coefficient in solution and factor ϵ accounts for the reduction of diffusion inside the membrane because of porosity and tortuosity effects. The thickness of the membrane, L_m, is used to normalize the position x across the membrane. The dimensionless electric potential, denoted by ϕ, can be converted to a dimensional voltage by multiplying it by RT/F, where F is the Faraday constant, R the universal gas constant, and T the temperature. To study MP rejection with NF membranes, we assume that the electrical potential across the membrane is only affected by

the transport of salt ions that are present at relatively high concentrations. Therefore, the concentrations and fluxes of salt ions across the membrane affect the rejection of MPs, but MPs do not affect the rejection and transport of ions. The aforementioned assumption enables us to define a transport parameter and derive a new expression for calculating MP rejection without compromising the model's accuracy while eliminating the need for complex numerical solutions.

The theory presented in this work is valid for a solution with monovalent ions and constant charge density across the membrane. Therefore, any effect of ions on the membrane charge is not considered. Considering these assumptions and integrating Eq. (1) from the feed solution – membrane boundary to the membrane – permeate solution boundary, we arrive at the following relation of the flux of a MP through the membrane

$$J_i = K_{\mathrm{f},i}\, k_{\mathrm{m},i}\, \mathrm{Pe}_{\mathrm{mod},i}\, \frac{c_{\mathrm{m,f},i}\exp(\mathrm{Pe}_{\mathrm{mod},i}) - c_{\mathrm{m,p},i}}{\exp(\mathrm{Pe}_{\mathrm{mod},i}) - 1} \tag{2}$$

of which a full derivation is given in the supplementary information (SI). Here, $c_{\mathrm{m,f},i}$ and $c_{\mathrm{m,p},i}$ are the concentrations of MPs just inside the membrane. Subscript f refers to the upstream (feed) side and subscript p to the downstream (permeate) side. We define a modified Peclet number $\mathrm{Pe}_{\mathrm{mod},i} = \frac{v_{\mathrm{w}}}{k_{\mathrm{m},i}} + z_i\phi_{\mathrm{m}}$, where ϕ_{m} corresponds to the difference in electrical potential across the membrane (upstream−downstream). For neutral MPs, Eq. (2) leads to the Hertz equation (Eq. 21 from [19]). We do not consider the effect of concentration polarization (CP) in the main calculations. However, in the SI, we present the corresponding equations including CP and illustrate the effect of CP on the rejection of MPs and NaCl. The concentration inside the membrane at both sides, feed and permeate, can be calculated based on the Donnan equilibrium. Using the feed side as an example, the concentration inside the membrane is given by

$$c_{\mathrm{m,f},i} = c_{\mathrm{f},i}\, \boldsymbol{\Phi}_i \exp^{(-z_i\phi_{\mathrm{f}})}. \tag{3}$$

The partitioning coefficient $\boldsymbol{\Phi}_i$ includes any contribution except for charge effects, and ϕ_{f} is the difference in electrical potential across the membrane–feed interface, which is a function of the membrane charge density, X, and the salt concentration at the membrane–feed interface. The membrane charge density can be positive or negative depending on the type of membrane. Moreover, the solution pH can affect the membrane charge and the ionization of solutes such as MPs or amphoteric ions. Models that consider the effect of pH on membrane charge and ionization degree of charged solutes can be found in literature [3,20,21] . Although, pH can strongly affect MP rejection [22], pH is close to pH = 7 in situations that are applicable for drinking water production, and therefore, in the experimental and theoretical sections of this work, pH is set to 7. In the case of a solution with a symmetric salt, ϕ_{f} is calculated as

$$\phi_{\mathrm{f}} = \mathrm{asinh}\left(\frac{X}{2\, c_{\mathrm{int},i}\, \boldsymbol{\Phi}}\right). \tag{4}$$

Considering the low water recovery limit, the concentration of MPs in the permeate is related to the MP flux by $c_{\mathrm{p},i} = J_i/v_{\mathrm{w}}$. In membrane modules, the low water recovery limit suggests that the concentration on the feed side, c_{f}, remains relatively constant along the channel. This limit is also valid in experimental conditions, such as when a membrane coupon is placed in a cross-flow cell for filtration experiments or in dead-end filtration experiments. Considering this relation and replacing $c_{\mathrm{m,f},i}$ in Eq. (2) we can define the flux of a MP as function of the concentration in the feed

$$J_i = P_i\, \mathrm{Pe}_{\mathrm{mod},i}\, \frac{v_{\mathrm{w}}\, c_{\mathrm{f},i}\, \alpha_{\mathrm{mod},i}\exp(-\mathrm{z_i}\phi_{\mathrm{f}})}{v_{\mathrm{w}}\,(\alpha_{\mathrm{mod},i} - 1) + P_i\, \mathrm{Pe}_{\mathrm{mod},i}\, \left(\exp(-\mathrm{z_i}\phi_{\mathrm{p}})\right)} \tag{5}$$

where $P_i = K_{\mathrm{f},i}k_{\mathrm{m},i}\boldsymbol{\Phi}_i$ is a empirical transport parameter (LMH) that depends on the properties of the MPs and the membrane that is used. For instance, the size of the MP and the porous structure of the membrane determine the mass transfer coefficient inside the membrane and the friction factor between the MP and the membrane matrix. Moreover, P_i is function of the partitioning coefficient, $\boldsymbol{\Phi}_i$, which can capture the effect of the membrane charge, the MP charge, and the solute–membrane interactions. The electrical potential at membrane–solution interface in the permeate side is given by ϕ_{p} is. Additionally, we define $\alpha_{\mathrm{mod},i} = \exp(\mathrm{Pe}_{\mathrm{mod,i}})$. The flux of charged MPs through the membrane is dependent on the electrical potential at the interface and across the membrane. This potential is intricately related to both the ionic strength and the transport of ions through the membrane. Consequently, to calculate MP transport and rejection, an accurate estimation of ion transport across the membrane is required. As part of the supplementary material for this work, we provide an Excel file and a manual for estimating the rejection of a monovalent salt with RO and NF membranes using the SF model [13]. The file employs a numerical solution and the Excel Solver extension to calculate salt rejection and the electrical potential values needed to estimate MP flux and rejection across the membrane.

Considering the low water recovery limit, rejection is given by

$$R_i = 1 - \frac{J_i}{c_{\mathrm{f},i}\, v_{\mathrm{w}}}. \tag{6}$$

By combining Eqs. (5) and (6), we have derived a new equation for MP rejection. This equation encompasses the key phenomena involved in MP rejection while maintaining simplicity through a limited set of model parameters. In the following sections, we evaluate the validity of this new equation by comparing model calculations with experimental data. The novel equation for MP rejection is then

$$R_i = 1 - P_i\, \mathrm{Pe}_{\mathrm{mod},i}\, \frac{\alpha_{\mathrm{mod},i}\exp(-\mathrm{z_i}\phi_{\mathrm{f}})}{v_{\mathrm{w}}\,(\alpha_{\mathrm{mod},i} - 1) + P_i\, \mathrm{Pe}_{\mathrm{mod},i}\, \left(\exp(-\mathrm{z_i}\phi_{\mathrm{p}})\right)}. \tag{7}$$

For neutral MPs, $\mathrm{Pe}_{\mathrm{mod},i}$ reduces to the conventional Peclet number $\mathrm{Pe}_i = v_{\mathrm{w}}/k_{\mathrm{m},i}$ and $\alpha_{\mathrm{Pe},i} = \exp(\mathrm{Pe}_i)$. Therefore, the rejection of a neutral MP is given by

$$R_i = 1 - P_i\, \mathrm{Pe}_i\, \frac{\alpha_{\mathrm{Pe},i}}{v_{\mathrm{w}}\,(\alpha_{\mathrm{Pe},i} - 1) + P_i\, \mathrm{Pe}_i}. \tag{8}$$

Eqs. (7) and (8), which are derived, for MP rejection with NF, are also applicable to RO membranes. These equations are based on the general ENP equation, which accounts for transport by diffusion, convection, and electromigration, and is applicable to RO membranes as well. The primary difference in MP rejection with RO membranes lies in the order of magnitude of the transport parameter and the mass transfer coefficient for the MPs. Additionally, in some cases, the equations presented in this work may be simplified for scenarios involving RO membranes, where convection and electromigration contribute less significantly to MP rejection.

2.2. Ion rejection

To calculate MP rejection, Eq. (7), one must know the electrical potential difference across the membrane, ϕ_{m}, and the potential at the feed, ϕ_{f}, and permeate, ϕ_{p}, interface, which are determined by the salt concentration, membrane charge density, and the transport of ions across the membrane. Therefore, an accurate model to predict ion flux and rejection is crucial. In this work, the SF model is employed to study the rejection of ions, incorporating the effects of leakage through the membrane resulting from imperfections.

The flux of ions through the membrane is calculated using Eq. (1), which, assuming mass conservation, $\frac{\partial c_i}{\partial x} = -\frac{\partial J_i}{\partial x}$, and steady state and no chemical reactions, $\frac{\partial c_i}{\partial t} = 0$, leads to

$$0 = K_{\mathrm{f},i}\, v_{\mathrm{w}}\frac{\partial c_i}{\partial x} - K_{\mathrm{f},i}k_{\mathrm{m},i}\frac{\partial}{\partial x}\left(\frac{\partial c_i}{\partial x} + z_i c_i \frac{\partial \phi}{\partial x}\right). \tag{9}$$

The concentration of ions inside the membrane at both sides, feed and permeate, are also calculated based on the Donnan equilibrium

Eq. (3). Furthermore, we consider local electroneutrality and zero electric current at all positions in the membrane according to

$$\sum_i z_i c_i + X = 0 \tag{10}$$

and

$$\sum_i z_i J_{m,i} = 0. \tag{11}$$

In the model for salt rejection, we include the effect of leakage through the membrane. Polymeric membranes do not have a uniform and perfect structure leading to imperfections that in practice behave as leakages (membrane sections with higher flux) [23,24]. Leakages through the membrane can also originate from physical damage of the polyamide layer during the experimental work [25], or by the pressure exerted by the spacers that are normally used in membrane configurations [26]. Therefore, we define the total flux of ions through the membrane, J_T, as the sum of the flux due to leakages, $J_{L,i}$, and across the intact membrane, $J_{m,i}$ which is given by Eq. (1). The flux due to leakages is defined as

$$J_{L,i} = A_L c_f \Delta P^{h,\infty} \tag{12}$$

where A_L is a permeability leakage factor in LMH/bar, $P^{h,\infty}$ is the pressure difference between feed and permeate [13]. Moreover, the total water flux including leakage, $v_{w,T}$, must be used to calculate the concentration of ions in the permeate according to $c_{p,i} = J_T/v_{w,T}$. In the SI, we present how the total water flux including leakage is calculated.

3. Materials and methods

3.1. Chemicals and membrane

The micropollutants used in this study are atrazine (ATZ), paracetamol (PCT), metformin (MTF), atenolol (ATN), sulfamethoxazole (SMX), ibuprofen (IBF), and aspirin (ASP). The properties of the MPs are provided in the supplementary information (SI). All chemicals were purchased in analytical grade with >98% purity. These MPs were selected for their diverse charges and their representation of a broad range of relevant MP sizes (129–266 g/mol). Selecting appropriate model compounds is essential for evaluating the influence of specific phenomena on MP rejection. With representative model compounds, valuable insights into the mechanisms driving MP rejection can be gained. Given our hypothesis that salt concentration impacts MP rejection based on charge, charge was a key factor in the selection. Size was also considered, as the significance of Donnan exclusion and electromigration varies with MP size. By working with these seven MPs, we aim to assess the effects of MP size and charge on rejection under different salt concentrations.

The commercial membrane NF270 (DOW-DuPont) was used in the filtration experiments. This polyamide thin film composite membrane has a molecular weight cut-off between 200–400 g/mol [27–30]. The NF270 was selected for this study because it is widely used for drinking water treatment and has been used in previous studies on MP removal and the effect of salt concentration. This enables a direct comparison of our results with existing data. The membrane was purchased from Lenntech, Delft, The Netherlands.

3.2. Filtration experiments

Filtration experiments were conducted to validate our model and to elucidate the impact of the sodium chloride (NaCl) concentration on the rejection of 7 MPs. The salt NaCl was used because of the anticipated weak interaction between MPs and the membrane with Na^+ and Cl^- ions. The experimental NaCl concentrations used during the experiments were 2, 5, 10, 50 and 100 mM and the concentration of MPs was set between 0.08 and 0.13 μM. Not all MPs were jointly tested in the same filtration experiment; instead, the MPs were divided into two groups.

- group 1: MTF (+) and ATN (+).
- group 2: ATZ, PCT, SMX (−), IBF (−), and ASP (−).

The experiments were performed using a cross-flow (lab-scale) membrane filtration system connected to two stainless steel membrane cells that were placed in series. The temperature of the feed solution was kept between T = 20–21 °C using a heat exchanger, and the pH of the feed solution was kept between pH = 6.8–7.2 by bubbling N_2 gas to control the N_2/CO_2 ratio in solution [31]. Membrane coupons of ~40 cm^2 of the membrane NF270 (DOW) were used. Coupons were cut after opening the spiral wound NF module. Before the filtration experiment, the coupons were soaked in deionized water for at least 24 h. Subsequently, the membrane was pretreated at high pressure (20 bar) for 4 h using deionized water.

Following the pretreatment with water, the filtration system was operated with the feed solution at pH = 7 for at least 24 h at 15 bar to ensure a steady state during the sampling. The same membrane coupons were consistently used throughout all experiments to avoid introducing other membranes with different degrees of imperfection that impact the leakage flux, $J_{L,i}$. During the experiments, we controlled the feed flow rate at 60 l/h while increasing the pressure from 2 to 10 bar. Following the adjustment of the pressure, we allowed the system to stabilize for a minimum of one hour before taking samples from the feed and permeate tanks. Every sample was analyzed to measure ion and MP concentrations and to calculate rejection.

3.3. Analytical methods

MP concentrations in the feed tank and permeate samples were measured to determine MP rejection. The MP measurement was done using an LC-MS/MS 6420 Triple Quad Mass Spectrometer (Agilent, USA) equipped with a UHPLC guard Zorbax Eclipse Plus C18 1.8 μm, 2.1 × 5 mm as pre-column and a Zorbax Eclipse Plus C18 RRHD 1.8 μm, 50 × 2.1 mm column (Agilent). For all MPs the same eluents were used except for ASP, which required different eluents for the analysis. The acid eluent (A) was a solution with neutral buffer of 10 mM ammonia, 10.4 mM formic acid, and 0.04 mM oxalic acid, and eluent B was methanol. For ASP analysis, eluent A was acetic acid (0.1%+) and eluent B was acetonitril. Detailed information regarding the ionization method, the precursor, product ions, and the time segment, are outlined in the SI.

4. Results

4.1. Salt rejection

The salt rejection was measured at 5 salt concentrations (2, 5, 10, 50, and 100 mM). In practical situations, the salt concentration may not reach values as high as 100 mM. However, this wide range of concentrations was chosen to have more confidence in the experimental results and the conclusions made about the effect of salt concentration on MP rejection. By evaluating such a wide range of salt concentrations, a significant effect on rejection could be observed and we could corroborate that our model is a good alternative to predict MP rejection. Moreover, the measurements of NaCl rejection were conducted to estimate model parameters that were used in this study and to determine the values of the electrical potential difference across the membrane, ϕ_m, and the potential at the feed, ϕ_f, and permeate, ϕ_p, interface for each salt concentration. Transport properties of Na^+ and Cl^- were fitted and estimated using experimental data; specifically, the friction factor, K_F, the mass transfer coefficient, k_m, and the partition coefficient Φ, which we assume to be the same for both ions. Furthermore, with the data for salt rejection, we also determined values for membrane charge density, X, water permeability, A_m, and the permeability leakage factor, A_L, which are parameters that depend on the membrane used during the experiments. In case a different membrane than the NF270 is used, it

Table 1
Model parameters that were estimated by fitting the experimental data for NaCl rejection.

Parameter	Value	Unit
K_f	0.065	–
Φ	1	–
X	−53	mM
L_m	100	nm
k_m	1040	LMH
A_m [a]	13.5	LMH/bar
A_L	1.1	LMH/bar

[a] A_m is the water permeability of the membrane and A_L is the permeability leakage factor.

would be necessary to identify the specific membrane and transport parameters that are characteristic of that membrane. However, the described theory is applicable to any NF membrane. The values of these parameters used in this work are given in Table 1. The water permeability, A_m, of the commercial NF270 membrane falls within the range reported in the literature (5.5–17 LMH/bar) for the NF270 membrane [29,30]. To compare the ion parameters listed in Table 1, we define a salt transport parameter, $P_{NaCl} = k_m \Phi K_f$, which has been established using a large set of experimental data for different RO membranes (0.015–0.95 LMH) [13]. In our study with NF, this transport parameter is two orders of magnitude larger than that for RO membranes, with a value of $P = 67.6$ LMH. This is consistent with the fact that NF membranes generally offer lower rejection than RO membranes.

Similarly, the ion parameters can be compared with those defined in the Spiegler and Kedem (SK) model, a classical version of the SF model. In the SK model, the reflection coefficient, σ, and the transport parameter, ω, are defined. These parameters relate to those in our model as follows: $\sigma = 1 - \Phi K_f$ and $\omega = k_m \Phi K_f$. In the present work, these values correspond to $\sigma = 0.935$ and $\omega = 67.6$ LMH. For the NF270 membrane, the reported ranges for the model parameters are $\sigma = 0.18 - 0.59$ and $\omega = 26 - 168$ LMH [32–36].

Fig. 2 depicts the results for salt rejection. The results show that salt concentration clearly affects rejection, which is in agreement with literature [37,38]. However, with the current model the data corresponding to the experiment with 50 mM NaCl was not accurately predicted. The model shows that the effect of salt concentration on rejection reaches a plateau at high concentration, and therefore the rejection with 50 mM and 100 mM are similar. These results are in line with previous studies on the effect of salt concentration on the rejection of monovalent salts [39,40]. However, experimentally the difference on rejection between these two concentrations is still significant. The values of the electrical potential difference across the membrane, ϕ_m, and the potential at the feed, ϕ_f, and permeate, ϕ_p, that were derived from the model calculations for salt rejection are necessary to estimate MP rejection. Since the experimental data corresponding to 50 mM NaCl was not accurately predicted, we include and analyze the removal of MPs with 50 mM NaCl separately in the SI.

4.2. MP rejection

The rejection of MPs was calculated using Eqs. (7) and (8) for charged and neutral MPs. In both cases, rejection is a function of the transport parameter P_i and the mass transfer coefficient k_m, which are characteristic of each MP and depend on the MP and membrane properties. In our model, these parameters were adjusted to have a good agreement between the experimental data and. The values for these parameters are given in Table 2. Besides, in the SI, we compare and discuss the values of these transport parameters based on MP properties, demonstrating their dependence on MP size and charge.

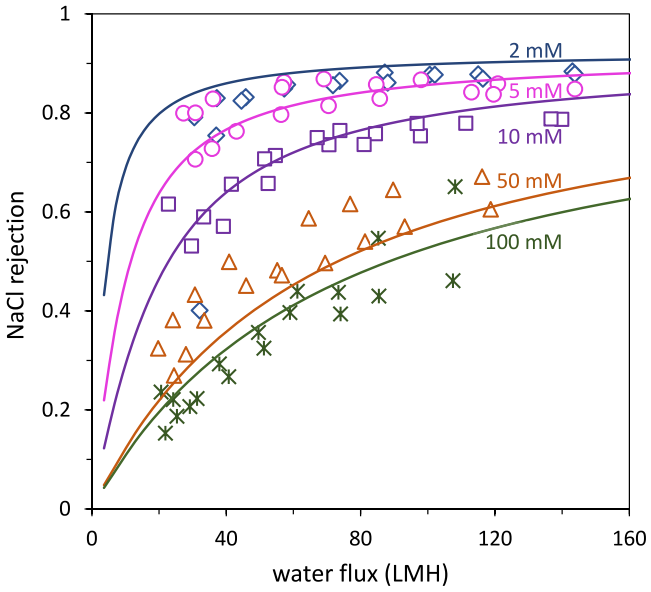

Fig. 2. Data and theory for salt rejection with different NaCl concentrations and water flux, v_w. The lines show the results from the model calculations. The parameters used in these calculations are given in Table 1.

Table 2
Model parameters that were used to calculate MP rejection with Eqs. (7) and (8).

Charge	Micropollutant	k_m (LMH)	P_i (LMH)
Neutral	Atrazine (ATZ)	190	4.5
Neutral	Paracetamol (PCT)	256	67
Positive	Metformin (MTF)	259	4.1
Positive	Atenolol (ATN)	173	3.4
Negative	Sulfamethoxazole (SMX)	189	7.1
Negative	Ibuprofen (IBF)	216	7.3
Negative	Aspirin (ASP)	238	8.6

4.2.1. Neutral MPs

In this study, we consider the effect of salt concentration on MP removal. Our model captures the impact of salt concentration on Donnan exclusion and electromigration inside the membrane. However, the effect of salt concentration on NF performance can go beyond these charge-based phenomena. For instance, increasing salt concentration can lead to pore swelling and lower the rejection of solutes [41–44]. High salt concentrations in the solution generally lead to a higher concentration of counter-ions inside the membrane. The presence of these counter-ions leads to a stronger repulsive force that can ultimately result in pore swelling. Experimentally, we observed that the rejection of neutral MPs (ATZ and PCT) is not influenced by the NaCl concentration. Therefore, with the experimental conditions of this study, we conclude that salt concentration only impacts MP rejection through charge-based phenomena.

In Fig. 3, the results for ATZ and PCT are depicted. The rejection of these MPs is solely determined by steric exclusion. Both experimental results and theoretical calculations indicate that the rejection of ATZ ($M_w \sim 215$ g/mol) is higher than of PCT ($M_w \sim 151$ g/mol). For paracetamol, the experimental results show significant deviation in rejection values, likely due to the limitations of the analytical method used. The small size and neutral charge of paracetamol present challenges for this method, which depends on fractionating molecules based on both polarity and size.

4.2.2. Charged MPs

The selection of micropollutants (MPs) plays a crucial role in studying and understanding the phenomena that impact MP rejection. In this study, we investigated and compared the effects of salt concentration

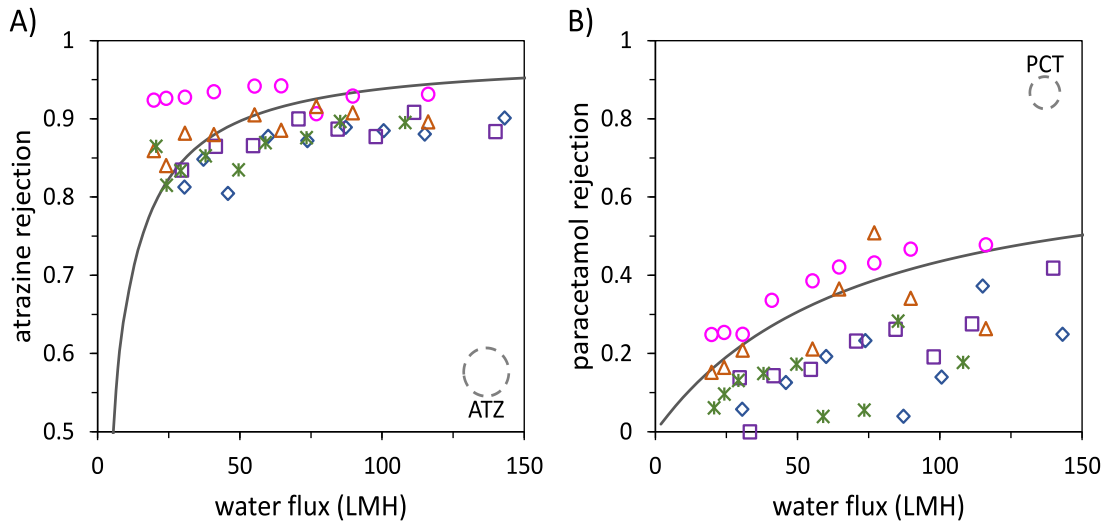

Fig. 3. Data and theory for the rejection of neutral MPs with different NaCl concentrations and water flux, v_w. (A) Rejection of atrazine (ATZ). (B) Rejection of paracetamol (PCT). The line shows the results from the model calculations. The markers represent the NaCl concentration: ◇ 2 mM, ○ 5 mM, □ 10 mM, △ 50 mM, and ∗ 100 mM. The model calculations are not dependent on the NaCl concentration, since the rejection of neutral MPs is not influenced by the NaCl concentration, Eq. (8). The parameters used in these calculations are given in Tables 1 and 2.

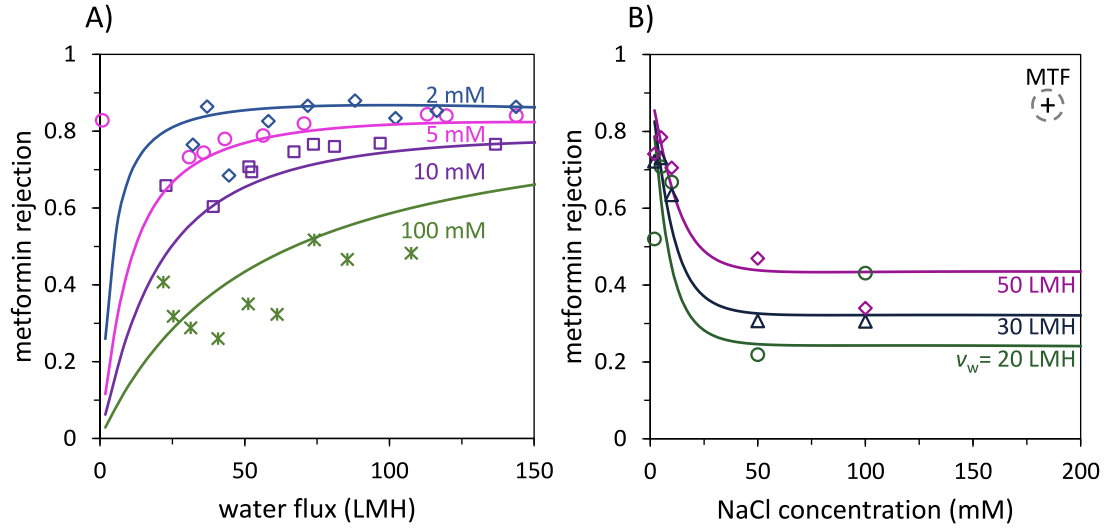

Fig. 4. Data and theory of metformin (MTF) rejection as function of the water flux, v_w, (A) and the NaCl concentration (B). The lines show the results from the model calculations using Eq. (7). The parameters used in these calculations are given in Tables 1 and 2.

on the rejection of positively and negatively charged MPs. Furthermore, we strategically chose MPs with varying sizes to determine whether salt concentration affects the rejection of small and large contaminants differently. This choice enables us to explore size-dependent rejection and, simultaneously, assess the potential interplay between size-based and charge-based effects in specific scenarios.

In the study of positively charged MPs, we examined MTF (M_w ~ 129 g/mol) and ATN (M_w ~ 266 g/mol). The results indicate distinct effects of salt concentration on the rejection of each MP. An increase in NaCl concentration has two significant impacts on rejection and transport mechanisms. Firstly, the decrease in the electrical potential at the feed interface, ϕ_f, diminishes the effect of Donnan exclusion of co-charged MPs and the attraction of counter-charged MPs. Secondly, the reduction in the electrical potential across the membrane, ϕ_m, influences the transport of charged MPs due to electromigration. For positively charged MPs, higher salt concentration leads to lower electrostatic attraction at the membrane–solution interface.

The data and calculations for MTF rejection as function of NaCl concentrations and water flux, v_w, are presented in Fig. 4. The rejection of MTF as function of v_w is given in Fig. 4A. The trend indicates that increasing NaCl concentration lowers MTF rejection. Given its small size and high mobility, with P_{MTF} = 4.08 LMH, MTF is minimally affected by lowering electrostatic attraction. This MP passes through the membrane, despite the Donnan effect, because of its small size. On the other hand, increasing NaCl concentration decreases electromigration which for positive MPs goes from permeate to feed, and therefore the rejection increases.

Furthermore, in Fig. 4B, the rejection of MTF is plotted as function of NaCl concentration for three values of water flux, v_w. The markers in this plot are interpolated values of rejection using the experimental data. The impact of NaCl concentration on the rejection of MTF diminishes with increasing NaCl concentration, reaching a plateau value after 50 mM NaCl. Similar behavior in rejection has been reported in studies investigating the effect of salt concentration on the rejection of single salts [39,40].

The case for ATN is somehow different from MTF. We observed that increasing NaCl concentration can have both effects, harm and improve ATN rejection. An increase in NaCl concentration from 2 to 5 mM

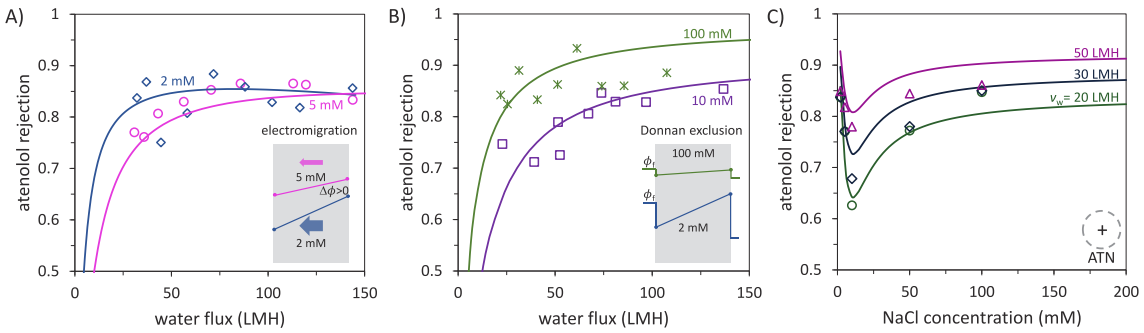

Fig. 5. Data and theory for atenolol (ATN) rejection as function of the NaCl concentration and water flux, v_w. (A) The rejection with 2 mM and 5 mM NaCl; in this case, rejection is decreased due to the higher electromigration. (B) ATN rejection with 10 and 100 mM NaCl; with these concentrations, ATN rejection increases with NaCl concentration due to the lower concentration of ATN inside the membrane. (C) ATN rejection as function of salt concentration. The parameters used in these calculations are given in Tables 1 and 2.

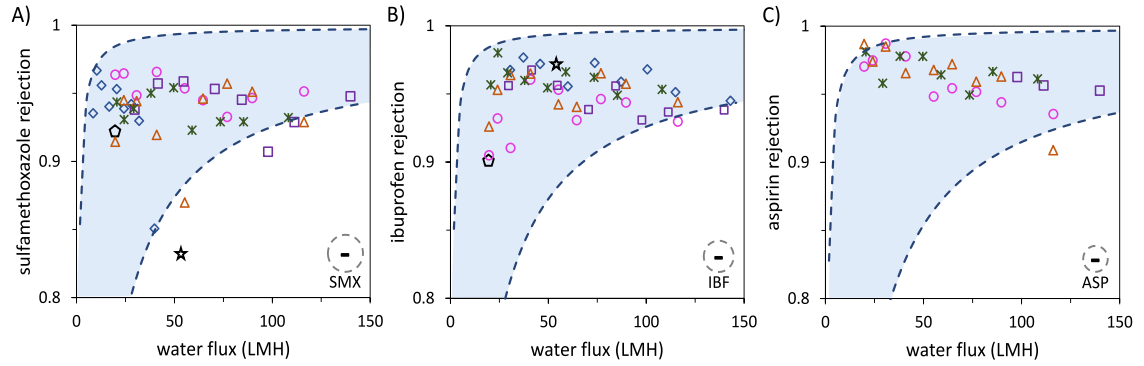

Fig. 6. Data and theory for the rejection of negatively charged MPs at different NaCl concentrations as function of water flux, v_w: (A) sulfamethoxazole (SMX), (B) ibuprofen (IBF), and (C) aspirin (ASP). The colored section corresponds to the rejection range calculated with 2 and 100 mM NaCl. The markers represent the NaCl concentration: ◇ 2 mM, ○ 5 mM, □ 10 mM, △ 50 mM, and ∗ 100 mM. Two data points from literature are included for comparison, these data points correspond to experimental work with membrane NF270 and similar operating conditions. The parameters used in these calculations are given in Tables 1 and 2. The data represented by a ⬠ is from Fujioka et al. (20 mM NaCl, pH = 8, and T = 20 °C) [45]. The data point represented by a ★ is from Nghiem et al. (20 mM NaCl, pH = 7, and T = 20 °C) [46].

results in lower rejection of ATN (Fig. 5A). In this concentration range, the effect of salt concentration on ATN rejection is dominated by electromigration. Although ATN is a larger molecule than MTF with a lower mobility within the membrane, P_{ATN} = 3.42 LMH, electromigration remains the dominating effect. However, this effect is counterbalanced by the Donnan effect at higher NaCl concentrations (Fig. 5B). The reduced electrostatic attraction, i.e., the reduction of electrical potential at the feed, ϕ_f, combined with the size exclusion of ATN decreases the concentration of ATN inside the membrane, according to Eq. (3). This, in turn, improves the rejection of ATN at NaCl concentrations higher than 5 mM.

In Fig. 5C, the rejection of ATN is depicted as function of salt concentration. It is shown that the rejection of ATN decreases to a minimum value within the NaCl concentration range of 9–12 mM. Further increases in NaCl concentration lead to higher rejections. These results for ATN illustrate the interplay between size effects and charge-based effects on MP rejection.

In this study, three negatively charged MPs were selected: SMX, IBF, and ASP. These MPs were used because they are representative of a wide size range [180–256 g/mol]. Based on previous studies [16,45], it was expected that salt concentration would have a weaker effect on the rejection of SMX and IBF, due to their large size. In the case of ASP, rejection can be more influenced by salt concentration because of the small size of this MP, i.e., the rejection of small MPs relies more on Donnan exclusion and electromigration. Based on our experimental results, we cannot conclude that salt concentration impacts the rejection of any of these negatively charged MPs, Fig. 6. We acknowledge some experimental limitations in our work; for instance, we could not use lower operating pressures. With pressures below 2 bar, the impact of the NaCl concentration on rejection would be more clear. Moreover, the analytical method used to measure the concentration of negatively charged MPs may not be sensitive enough at high salt concentrations due to the interference of the water matrix during the measurements or the further dilution that was needed for the samples.

Compared to the experimental data, our model predicts that increasing salt concentration leads to a small decrease in the rejection of all three MPs. In Fig. 6, instead of presenting the model results for each NaCl concentration we show a range of rejection that corresponds to the model results with 2 (upper limit) and 100 (lower limit) mM NaCl. Although the model does not predict the data perfectly, it provides a good qualitative description of the data. Therefore, we still believe that the model proposed in this work to estimate the rejection of MPs, Eqs. (7) and (8), is a useful and accurate model, especially because the model captures the main mechanism involved in the rejection of MPs but remains easy to be implemented with only a few model parameters that can be found experimentally. Furthermore, we compared our model prediction and experimental data for SMX and IBF rejection with the work of Nghiem et al. [46] and Fujioka et al. [45]. Their experimental results are similar to ours, with IBU rejection between 90%–97% and SMX rejection between 83%–92%. These values fall in the rejection range predicted by our model.

5. Conclusions

We derived a new model to study the rejection of MPs with NF membranes that is derived from the SF model. This model captures the main mechanisms influencing MP rejection with NF, namely convection, diffusion, and electromigration. Moreover, the implementation of the model remains simple due to the reduced number of parameters needed to estimate MP rejection. The mass transfer coefficient $k_{m,i}$

and the transport parameter P_i for each micropollutant can be easily identified for specific membranes, provided that the rejection of ions and the membranes properties are known.

Additionally, we present a robust experimental dataset that was used to validate the model described in this work. The results from our model are in agreement with the experimental data. However, for the implementation of this model, one must know the membrane's performance in terms of salt rejection and identify key membranes properties such as the membrane charge density.

Experimentally, we used several NaCl concentrations to investigate the effect of water composition on the rejection of MPs with different properties. We found that effect of salt concentration on MP rejection depends on MP charge and size. In the case of counter-charged and small MPs (MTF), high salt concentrations increase electromigration of MPs across the membrane which reduces rejection significantly. On the other hand, with counter-charged and large MPs (ATN), high salt concentration can increase rejection due to a lower electrostatic attraction of ATN by the membrane, resulting in a lower MP concentration and transport inside the membrane. Experimentally, we could not conclude whether the rejection co-charged MPs (SMX, IBF, and ASP) is strongly influenced by salt concentration. However, our model provides a good qualitative description of experimental data.

CRediT authorship contribution statement

S. Castaño Osorio: Writing – original draft, Methodology, Conceptualization. **I.I. Ryzhkov:** Writing – review & editing, Methodology, Conceptualization. **E. Spruijt:** Writing – review & editing, Methodology, Conceptualization. **A. van der Wal:** Writing – review & editing, Funding acquisition. **P.M. Biesheuvel:** Writing – review & editing, Methodology, Conceptualization. **J.E. Dykstra:** Writing – review & editing, Supervision, Resources, Project administration, Methodology, Funding acquisition, Conceptualization.

Declaration of competing interest

The authors declare that they have no known competing financial interests or personal relationships that could have appeared to influence the work reported in this paper.

Data availability

Data will be made available on request.

Acknowledgments

This work was performed in the cooperation framework of Wetsus, European centre of Excellence for Sustainable Water Technology (www.wetsus.nl). Wetsus is co-funded by the Dutch Ministry of Economic Affairs and Ministry of Infrastructure and Environment, the Province of Fryslân, the Northern Netherlands Provinces, and The Netherlands Organization for Scientific Research. The authors like to thank the participants of the Advanced Water Treatment theme for fruitful discussion and financial support.

Appendix A. Supplementary data

Supplementary material related to this article can be found online at https://doi.org/10.1016/j.memsci.2024.123347.

References

[1] B. Peñate, L. García-Rodríguez, Current trends and future prospects in the design of seawater reverse osmosis desalination technology, Desalination 284 (2012) 1–8.
[2] Y.J. Lim, K. Goh, M. Kurihara, R. Wang, Seawater desalination by reverse osmosis: Current development and future challenges in membrane fabrication – A review, J. Membr. Sci. 629 (2021) 119292.
[3] P.M. Biesheuvel, L. Zhang, P. Gasquet, B. Blankert, M. Elimelech, W.G. van der Meer, Ion selectivity in brackish water desalination by reverse osmosis: theory, measurements, and implications, Environ. Sci. Technol. Lett. 7 (2019) 42–47.
[4] R. Xu, W. Qin, Z. Tian, Y. He, X. Wang, X. Wen, Enhanced micropollutants removal by nanofiltration and their environmental risks in wastewater reclamation: A pilot-scale study, Sci. Total Environ. 744 (2020) 140954.
[5] S. Castaño Osorio, P.M. Biesheuvel, E. Spruijt, J.E. Dykstra, A. van der Wal, Modeling micropollutant removal by nanofiltration and reverse osmosis membranes: considerations and challenges, Water Res. 225 (2022) 119130.
[6] T. Kim, J.E. Drewes, R. Scott Summers, G.L. Amy, Solute transport model for trace organic neutral and charged compounds through nanofiltration and reverse osmosis membranes, Water Res. 41 (2007) 3977–3988.
[7] L.D. Nghiem, A.I. Schäfer, M. Elimelech, Removal of natural hormones by nanofiltration membranes: Measurement, modeling, and mechanisms, Environ. Sci. Technol. 38 (2004) 1888–1896.
[8] X. Wang, B. Li, T. Zhang, X. yan Li, Performance of nanofiltration membrane in rejecting trace organic compounds: Experiment and model prediction, Desalination 370 (2015) 7–16.
[9] A.R.D. Verliefde, E.R. Cornelissen, S.G.J. Heijman, J.Q.J.C. Verberk, G.L. Amy, B. van der Bruggen, J.C. van Dijk, Construction and validation of a full-scale model for rejection of organic micropollutants by NF membranes, J. Membr. Sci. 339 (2009) 10–20.
[10] A.R.D. Verliefde, E.R. Cornelissen, S.G.J. Heijman, E.M.V. Hoek, G.L. Amy, B. van der Bruggen, J.C. van Dijk, Influence of solute-membrane affinity on rejection of uncharged organic solutes by nanofiltration membranes, Environ. Sci. Technol. 43 (2009) 2400–2406.
[11] L. Ma, L. Gutierrez, M. Vanoppen, D.N. Lorenz, C. Aubry, A. Verliefde, Transport of uncharged organics in ion-exchange membranes: experimental validation of the solution-diffusion model, J. Membr. Sci. 564 (2018) 773–781.
[12] S. Botton, A.R. Verliefde, N.T. Quach, E.R. Cornelissen, Influence of biofouling on pharmaceuticals rejection in NF membrane filtration, Water Res. 46 (2012) 5848–5860.
[13] P.M. Biesheuvel, S.B. Rutten, I.I. Ryzhkov, S. Porada, M. Elimelech, Theory for salt transport in charged reverse osmosis membranes: Novel analytical equations for desalination performance and experimental validation, Desalination 557 (2023) 116580.
[14] J. Cuhorka, E. Wallace, P. Mikulášek, Removal of micropollutants from water by commercially available nanofiltration membranes, Sci. Total Environ. 720 (2020) 137474.
[15] J. Luo, Y. Wan, Effects of pH and salt on nanofiltration—a critical review, J. Membr. Sci. 438 (2013) 18–28.
[16] L.D. Nghiem, A.I. Schäfer, M. Elimelech, Role of electrostatic interactions in the retention of pharmaceutically active contaminants by a loose nanofiltration membrane, J. Membr. Sci. 286 (2006) 52–59.
[17] S.B. Rutten, M.A. Junker, L.H. Leal, W.M. de Vos, R.G. Lammertink, J. de Grooth, Influence of dominant salts on the removal of trace micropollutants by hollow fiber nanofiltration membranes, J. Membr. Sci. 678 (2023) 121625.
[18] M.N. Fini, H.T. Madsen, J. Muff, The effect of water matrix, feed concentration and recovery on the rejection of pesticides using NF/RO membranes in water treatment, Sep. Purif. Technol. 215 (2019) 521–527.
[19] P.M. Biesheuvel, S. Porada, M. Elimelech, J.E. Dykstra, Tutorial review of reverse osmosis and electrodialysis, J. Membr. Sci. 647 (2022) 120221.
[20] E. Virga, E. Spruijt, W.M. de Vos, P.M. Biesheuvel, Wettability of amphoteric surfaces: the effect of pH and ionic strength on surface ionization and wetting, Langmuir 34 (2018) 15174–15180.
[21] P.M. Biesheuvel, W.S. de Lint, Application of the charge regulation model to the separation of ions by hydrophilic membranes, J. Colloid Interface Sci. 241 (2001) 422–427.
[22] L.D. Nghiem, A.I. Schäfer, M. Elimelech, Role of electrostatic interactions in the retention of pharmaceutically active contaminants by a loose nanofiltration membrane, J. Membr. Sci. 286 (2006) 52–59.
[23] T.E. Culp, B. Khara, K.P. Brickey, M. Geitner, T.J. Zimudzi, J.D. Wilbur, S.D. Jons, A. Roy, M. Paul, B. Ganapathysubramanian, et al., Nanoscale control of internal inhomogeneity enhances water transport in desalination membranes, Science 371 (2021) 72–75.
[24] G.M. Geise, Why polyamide reverse-osmosis membranes work so well, Science 371 (2021) 31–32.
[25] D. Venkataswamy Gowda, D. Harmsen, A. D'Haese, E.R. Cornelissen, Membrane integrity monitoring on laboratory scale: Impact of test cell-induced damage on membrane selectivity, J. Membr. Sci. 669 (2023) 121281.

[26] C. Lee, I.S. Kim, Osmotic membrane under spacer-induced mechanical compression: Performance evaluation and 3D mechanical simulation for module optimization, J. Membr. Sci. 641 (2022) 119875.
[27] B.M. Xaba, S.J. Modise, B.J. Okoli, M.E. Monapathi, S. Nelana, Characterization of selected polymeric membranes used in the separation and recovery of palladium-based catalyst systems, Membranes 10 (2020) 166.
[28] M. Dalwani, N.E. Benes, G. Bargeman, D. Stamatialis, M. Wessling, A method for characterizing membranes during nanofiltration at extreme pH, J. Membr. Sci. 363 (2010) 188–194.
[29] A. Ramdani, A. Deratani, S. Taleb, N. Drouiche, H. Lounici, Performance of NF90 and NF270 commercial nanofiltration membranes in the defluoridation of Algerian brackish water, Desalination Water Treat. 212 (2021) 286–296.
[30] O.P. Crossley, R.B. Thorpe, D. Peus, J. Lee, The effect of salinity on the pressure susceptibility of the NF270 membrane, Desalination 564 (2023) 116804.
[31] M. Pranić, E.M. Kimani, P.M. Biesheuvel, S. Porada, Desalination of complex multi-ionic solutions by reverse osmosis at different pH values, temperatures, and compositions, ACS Omega 6 (2021) 19946–19955.
[32] H. Kelewou, A. Lhassani, M. Merzouki, P. Drogui, B. Sellamuthu, Salts retention by nanofiltration membranes: Physicochemical and hydrodynamic approaches and modeling, Desalination 277 (2011) 106–112.
[33] R.R. Nair, E. Protasova, S. Strand, T. Bilstad, Implementation of Spiegler–Kedem and steric hindrance pore models for analyzing nanofiltration membrane performance for smart water production, Membranes 8 (2018) 78.
[34] H. Al-Zoubi, W. Omar, Rejection of salt mixtures from high saline by nanofiltration membranes, Korean J. Chem. Eng. 26 (2009) 799–805.
[35] N. Zouhri, M. Igouzal, M. Larif, M. Hafsi, M. Taky, A. Elmidaoui, Prediction of salt rejection by nanofiltration and reverse osmosis membranes using Spiegler-Kedem model and an optimisation procedure, Desalination Water Treat. 120 (2018) 41–50.
[36] S. Bason, O. Kedem, V. Freger, Determination of concentration-dependent transport coefficients in nanofiltration: Experimental evaluation of coefficients, J. Membr. Sci. 326 (2009) 197–204.
[37] L. Han, J. Tian, C. Liu, J. Lin, J.W. Chew, Influence of pH and NaCl concentration on boron rejection during nanofiltration, Sep. Purif. Technol. 261 (2021) 118248.
[38] J. Tanninen, M. Mänttäri, M. Nyström, Effect of salt mixture concentration on fractionation with NF membranes, J. Membr. Sci. 283 (2006) 57–64.
[39] S. Bandini, C. Mazzoni, Modelling the amphoteric behaviour of polyamide nanofiltration membranes, Desalination 184 (2005) 327–336.
[40] Z. Wang, K. Xiao, X. Wang, Role of coexistence of negative and positive membrane surface charges in electrostatic effect for salt rejection by nanofiltration, Desalination 444 (2018) 75–83.
[41] X. Wang, C. Zhang, P. Ouyang, The possibility of separating saccharides from a NaCl solution by using nanofiltration in diafiltration mode, J. Membr. Sci. 204 (2002) 271–281.
[42] M. Nilsson, G. Trägårdh, K. Östergren, The influence of pH, salt and temperature on nanofiltration performance, J. Membr. Sci. 312 (2008) 97–106.
[43] A. Escoda, P. Fievet, S. Lakard, A. Szymczyk, S. Déon, Influence of salts on the rejection of polyethyleneglycol by an NF organic membrane: Pore swelling and salting-out effects, J. Membr. Sci. 347 (2010) 174–182.
[44] J. Luo, Y. Wan, Effect of highly concentrated salt on retention of organic solutes by nanofiltration polymeric membranes, J. Membr. Sci. 372 (2011) 145–153.
[45] T. Fujioka, S.J. Khan, J.A. McDonald, L.D. Nghiem, Nanofiltration of trace organic chemicals: A comparison between ceramic and polymeric membranes, Sep. Purif. Technol. 136 (2014) 258–264.
[46] L.D. Nghiem, A.I. Schäfer, M. Elimelech, Pharmaceutical retention mechanisms by nanofiltration membranes, Environ. Sci. Technol. 39 (2005) 7698–7705.